

Liquid phase bonding of yttria stabilized zirconia with CaO–TiO₂–SiO₂ glass

BI-SHIOU CHIOU

*Department of Electronic Engineering and Institute of Electronics,
National Chiao Tung University, Hsinchu, Taiwan*

CHUNG-DAW YOUNG, JENQ-GONG DUH

Department of Materials Science and Engineering, National Tsing Hua University, Hsinchu, Taiwan

A 36.8 wt % CaO–26.2 wt % TiO₂–37.0 wt % SiO₂ glass (CTS) was employed as the ceramic brazer for the bonding of 3 mol % yttria stabilized zirconia (YSZ3). Sandwich-like YSZ3–CTS–YSZ3 specimens were fabricated and temperature dependence of the bonding strength was evaluated. An optimum bonding process was achieved at a bonding temperature of 1424 °C for 30 min with CTS glass slurry having a glass/organic ratio of 1.82. The effects of processing parameters on the bonding was investigated on the basis of the metallurgical evolution at the interface. In addition, predominating factors affecting the bonding strength were also explored.

1. Introduction

For the application of advanced ceramics at elevated operating temperatures, high strength and good chemical stability are of practical importance. To make use of these properties, it is essential to find appropriate joining methods concerning the bonding of ceramics. One common method of joining ceramics is brazing. Brazing is performed by melting a filler material to join materials of higher melting points. The filler material can be metal [1–5], alloy [6–10], or ceramic [11–17]. The brazed joints made with metallic alloy have relatively high strength at room temperature, however, their strength at elevated temperatures is limited because of the relatively low softening temperature of the alloy braze material. Hence, the use of a ceramic filler for the bonding of ceramic should allow for increased joint strengths at high temperature. Good bonding strength is possible if the filler material wet and/or reacts with the ceramic to be joined.

The purpose of this research is to study the liquid phase bonding of 3 mol % yttria stabilized zirconia with CaO–TiO₂–SiO₂ glass. Filler compositions in the CaO–TiO₂–SiO₂ systems were previously used to join ceramics, such as silicon nitride and MgO partially stabilized zirconia [14]. This CaO–TiO₂–SiO₂ system was comprehensively studied by Devriess *et al.* [18]. There are 17 invariant points in the ternary system. The composition selected as filler material in this study is a eutectic composition consisting of 36.8 wt % CaO–26.2 wt % TiO₂–37.0 wt % SiO₂, which has a melting temperature of 1348 °C. The YSZ3 is chosen for its high fracture toughness, which is hardly affected by the thermal cycling [19, 20]. In this study, the thermal properties of CTS glass was first evaluated, and the reaction between CTS

glass and YSZ3 was characterized to investigate the bonding behaviour.

2. Experimental procedures

Yttria stabilized zirconia, with composition 3 mol % Y₂O₃–ZrO₂ (YSZ3) was selected as the matrix material. The YSZ3 powder (Toyo Soda Co., Tokyo) has an average particle size of 0.3 µm, a specific surface area of 18 m² g⁻¹, and a crystallite size around 24 nm. Samples of YSZ3, with 4 × 3 × 34 mm³ in dimension, were prepared by sintering at 1500 °C for 3 h. The sintered density was 6.01 g cm⁻³ (i.e. 98.9 % theoretical density) as measured by Archimedes' method.

For the preparation of CTS glass, appropriate amounts of CaCO₃, SiO₂, and TiO₂ (reagent grade) were mixed in alcohol with ZrO₂ balls in a Teflon jar for 24 h. The mixed powders were then dried and melted at 1500 °C for 1 h in a Pt crucible. The melt was quenched into iced deionized water to form glass frits. The frits were ground with Al₂O₃ mortar and pestle into powders and then sieved to pass through 325 mesh. The sieved powders were blended with a viscous organic vehicle consisting of 70 wt % N-200 ethyl cellulose in butyl carbitol solvent to form a glass slurry with various glass powder/organic ratios (p/o). The slurry was then blended with a two-roll mill to obtain a homogeneous mixture. Part of the melt was quenched into a Cu mould to form a glass block. The amorphous structure of the glass was investigated by X-ray diffraction technique (XRD). Thermal expansion of the glass was measured with an automatic recording dilatometer (ULVAC DL-1500) at a heating rate of 10 °C min⁻¹ until softening of the glass occurred. Differential thermal analysis (DTA) of the glass

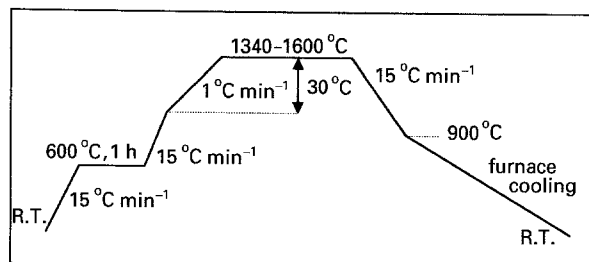


Figure 1 Temperature profile for the bonding of YSZ3-CTS-YSZ3 assembly. R.T., room temperature.

powder was carried out with a thermogravimetric analyser (ULVAC TGD-5000).

For the bonding experiment, two zirconia discs were joined with glass slurry and dried at 150 °C to form a sandwich assembly with an interlayer thickness of about 0.5 mm. The specimens were then placed vertically in an Al₂O₃ crucible and heated to a peak temperature ranging from 1340 °C to 1600 °C. The heating profile for the specimens is given in Fig. 1. The bonded zirconia were then ground with SiC papers from No. 120 up to 600. The bonding strength was measured by the three point bending method and was calculated as follows

$$\sigma_{3P} = \frac{3LP}{2t^2W} \quad (1)$$

where L , t , and W are the sample length, thickness, and width, respectively. P is the load applied when fracture occurs. The standard deviation of the bending strength was then calculated

$$S = \left[\frac{\sum \sigma_{3P}^2 - (\sum \sigma_{3P})^2/n}{n-1} \right]^{1/2} \quad (2)$$

where n is the number of specimens tested. The phases and morphology of the fractured surface were analysed with X-ray diffractometer (D/MAX-B, Rigaku, Japan) and EPMA (JXA-733, Jeol, Japan), respectively. The microstructure and compositions around the joint were investigated by transmission electron microscopy (TEM) (JEM-2000 FX, Jeol, Japan) and EDX (AN10000, LINK, UK).

3. Results and Discussion

3.1. Thermal properties of CaO-TiO₂-SiO₂ (CTS) glass

The thermal expansion of CTS glass as a function of temperature is shown in Fig. 2. The transition temperature and softening temperature of the glass are around 750 °C and 800 °C, respectively. The coefficient of thermal expansion (CTE) from room temperature to 640 °C is around $8.42 \times 10^{-6} \text{ °C}^{-1}$. In the differential thermal analysis (DTA) of the glass powder, an exothermic peak at around 873 °C is observed before the melting of the glass at around 1330 °C, as shown in Fig. 3. Upon cooling, three exothermic peaks appear at 1260 °C, 1134 °C, and 1095 °C, respectively. To study the reaction associated with the 873 °C exothermic peak, bulk CTS glass was then heated at 900 °C for 8 h. The XRD pattern, given in Fig. 4, shows the presence of the crystalline Ca₃Ti₂O₇ and CaSiO₃ (parawollastonite). This suggests that the

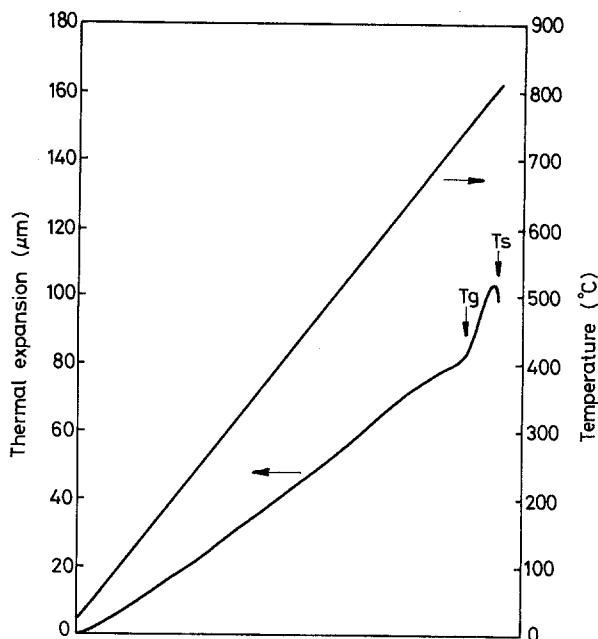


Figure 2 Thermal expansion of 36.8 wt % CaO-26.2 wt % TiO₂-37.0 wt % SiO₂ glass bulk. Sample heating rate 10 °C min⁻¹.

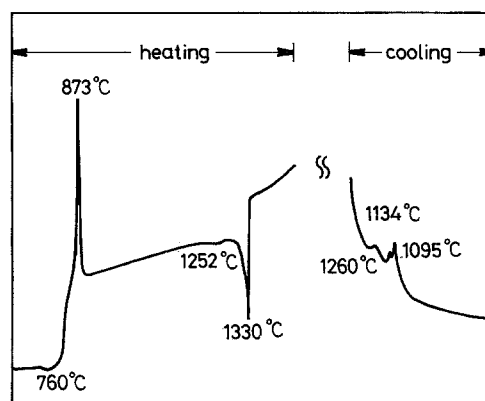


Figure 3 Differential thermal analysis (DTA) of 36.8 wt % CaO-26.2 wt % TiO₂-37.0 wt % SiO₂ glass powder.

bulk glass crystallizes after 8 h heat treatment at 900 °C, and three exothermic peaks observed in the DTA result of the glass powder, as shown in Fig. 3, may correspond to precipitation of the three crystalline phases in the transient state.

The crystallization of the CTS glass provides a promising candidate for the filler material for ceramic bonding. In the initial stage of the bonding process, the CTS glass flows to wet the substrate and the so-called liquid phase bonding proceeds. The glass then crystallizes and reacts with the substrate to form a ceramic composite, which, hopefully, is a highly refractory material. The joint thus formed should have a high bonding strength at elevated temperatures.

The thermal expansion coefficients of YSZ3, CTS glass and crystallized CTS ceramic are $9.74 \times 10^{-6} \text{ °C}^{-1}$ (25–900 °C), $8.42 \times 10^{-6} \text{ °C}^{-1}$ (25–640 °C), and $8.85 \times 10^{-6} \text{ °C}^{-1}$ (25–900 °C), respectively. The stress σ_α caused by the thermal mismatch can be estimated as follows

$$\sigma_\alpha = E\varepsilon \quad (3)$$

$$\varepsilon = \Delta\alpha \cdot \Delta T \quad (4)$$

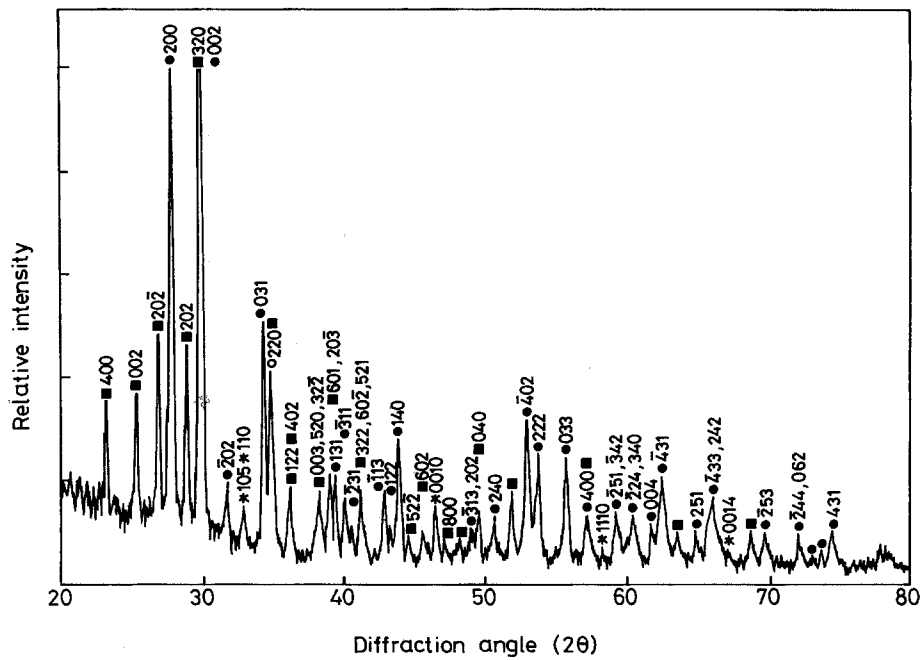


Figure 4 X-ray diffraction patterns of 36.8 wt % CaO–26.2 wt % TiO₂–37.0 wt % SiO₂ glass bulk heat treated at 900 °C for 8 h. *, Ca₃Ti₂O₇; ●, CaTiSiO₅; ■, CaSiO₃.

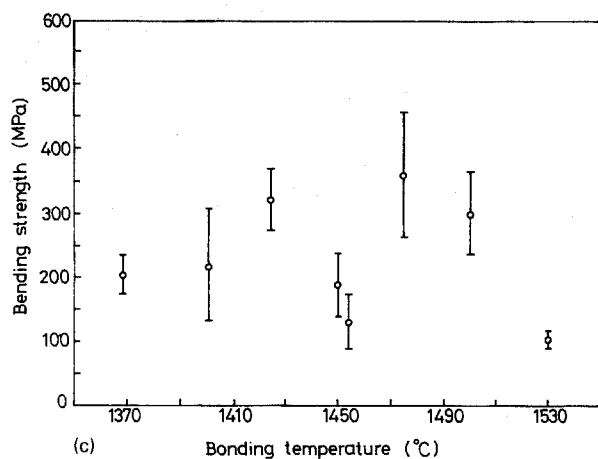
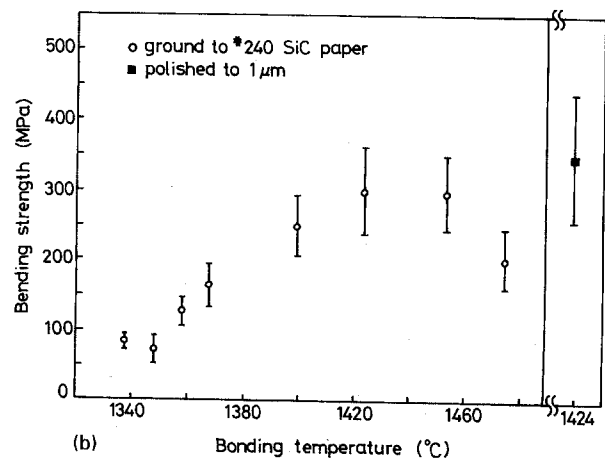
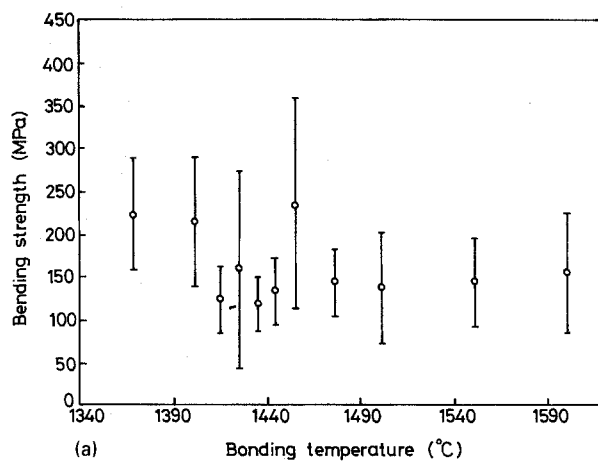


Figure 5 The temperature dependence of the bending strength of YSZ3–CTS–YSZ3 assembly. Bonding time: 30 min, glass powder/organic ratio (p/o) (a) p/o < 1; (b) p/o = 1.82, ○, ground to 240 SiC paper; ■, polished to 1 μm; and (c) p/o = 3.17.

where $\Delta\alpha$ is the CTE difference between YSZ3 and CTS ceramic. ΔT is 875 °K, ε is strain, E is 2.04×10^4 kgfmm⁻², which is Young's modulus of YSZ3. The stress σ_a developed in the YSZ3 as a result of the thermal expansion difference is 158 MPa. Lange

[21] estimated that the tetragonal form of pure zirconia may be retained by an external hydrostatic pressure greater than 3.7 GPa. The amount of constraint required decreased with the increase in stabilizing oxide content. However, how much tensile stress would be applied to induce the tetragonal to monoclinic ($t \rightarrow m$) phase transformation was not mentioned because the t -ZrO₂ particle would be stabilized in other ceramic matrices not only by reducing the particle–matrix thermal expansion mismatch to decrease the thermal stress, but also by optimizing the processing parameters, such as: particle size, concentration of stabilizer, driving force for the transformation, volumes fraction of ZrO₂ etc. [22]. Hence, for the present stage, it is difficult to predict whether 158 MPa is sufficient to induce the $t \rightarrow m$ transformation.

3.2. Bending strength and fracture surface morphology

A series of bonding test were performed for YSZ3-CTS-YSZ3 assembly at various temperatures for glass slurry with various CTS powder-to-organic ratio (p/o). Fig. 5 gives the bending strength of the assembly as a function of temperature for samples with p/o ranges from less than 1 to 3.17. It should be pointed out that appreciable scattering of the bending strength data is obtained for samples using a brazer with $p/o < 1$. Fig. 6 gives the fracture surface for the sample with $p/o < 1$ bonded at 1348 °C. Unwetted regions are observed on the fractured surface for samples with a low glass concentration slurry (i.e. $p/o < 1$), because the amount of glass slurry is not enough to cover the entire joint interface after bonding. The bonding strength thus derived is not based on the real contact area, and consequently, a large deviation is obtained.

On the basis of X-ray mapping results exhibited in Fig. 6(c-g), the wetted regions are enriched in Ca, Ti, and Si, while the unwetted regions are Zr and Y rich. In the unwetted region the grains near the boundary are larger than those near the centre. Similar phenomena

prevail in samples bonded at other temperatures. It is argued that the glassy liquid phase, which provides a faster atomic diffusion path than the concurrent solid state process, enhances the sintering of zirconia.

In the case of $p/o = 1.82$, the bending strength increases initially with the bonding temperature, reaches a peak value around 1424 °C and decreases afterwards, as indicated in Fig. 5(b). However, for samples bonded with $p/o = 3.17$, no simple relationship between bending strength and temperature is observed.

Fig. 7(a) is the bright field image of bonded zirconia matrix located within 0.5 mm from the joint. Fig. 7(b-d) are the corresponding patterns of the grain indicated by an arrow and show the monoclinic spot splitting. The monoclinic spot splitting in Fig. 7(b) represents the $[01\bar{1}]$ projection twinned on the (100) plane. The orientation relation in terms of the tetragonal phase are $[01\bar{1}]_t \parallel [01\bar{1}]_m$ and $(100)_t \parallel (100)_m$ with twinning on $(100)_m$. As referred to in Hannink's work [23], in which the tetragonal cell was considered as a slightly distorted cube, the averaged specimens with 8.4 mol % CaO-ZrO₂ showed a similar spot splitting type. It was reported that the

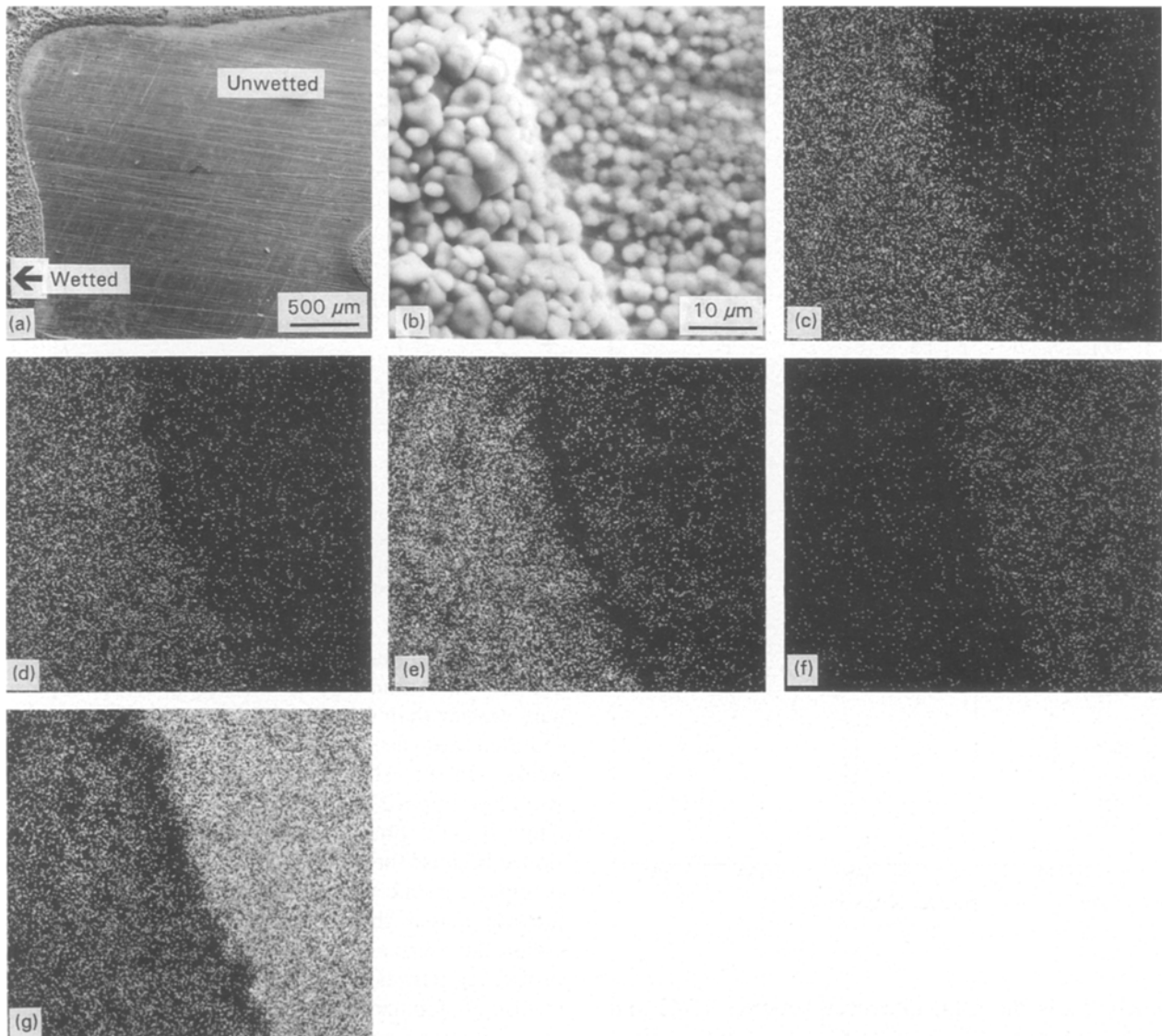


Figure 6 Fracture surface of sample bonded with glass slurry $p/o < 1$ at 1348 °C. (a) SEM micrograph; (b) SEM micrograph of a region across the wetted and unwetted region; (c) Ca X-ray mapping; (d) Ti X-ray mapping; (e) Si X-ray mapping; (f) Y X-ray mapping; (g) Zr X-ray mapping of region in (b).

tetragonal-to-monoclinic transformation occurred without appreciable lattice rotation and thus the simple cube-to-cube relationships with the added distortion due to the $t \rightarrow m$ transformation were observed. Fig. 7c and d indicate $\{112\}$ and $\{210\}$ selected area diffraction patterns, respectively, and seem to coincide with the variants of spots from $t \rightarrow m$ transformation and twin spots of the monoclinic phase. Similar patterns are found in the sample bonded at 1454°C as shown in Fig. 8a–c. Results of energy dispersive X-ray analysis (EDX) in the grain and grain boundary triple point are given in Table I. The elements Ca and Si appear to exist in the grain boundary triple point and no solid solution with ZrO_2 is ever observed. However, it seems that Ti has the tendency to be dissolved into the ZrO_2 grains from the grain boundary triple points. In addition, Y contents in the grain for the sample bonded at 1454°C decrease

to zero, while about 2 mol % Ti are found in the ZrO_2 matrix. The increase of Ti content and the decrease of Y content in ZrO_2 matrix must be implicated in the $t \rightarrow m$ phase transformation. It is argued that the existence of Ti in ZrO_2 matrix will destabilize the tetragonal phase and enhance the $t \rightarrow m$ phase transformation. A similar case was reported by Agrawal *et al.* [24] in which increasing amounts of titania reduced the amounts of the cubic phase, which was destabilized by addition of titania, and resulted in the increasing of the monoclinic phase fraction.

The possible reaction between CTS glass and zirconia can be probed from another microscopic viewpoint. The ionic radius of Ti^{4+} , Zr^{4+} and Ca^{2+} are 0.068 nm, 0.079 nm and 0.0893 nm, respectively [25]. In Ramaswamy's work [26], the lattice parameter of the cubic phase increased with the increase of the amount of CaO in the ZrO_2 –CaO sample. In Agrawal's

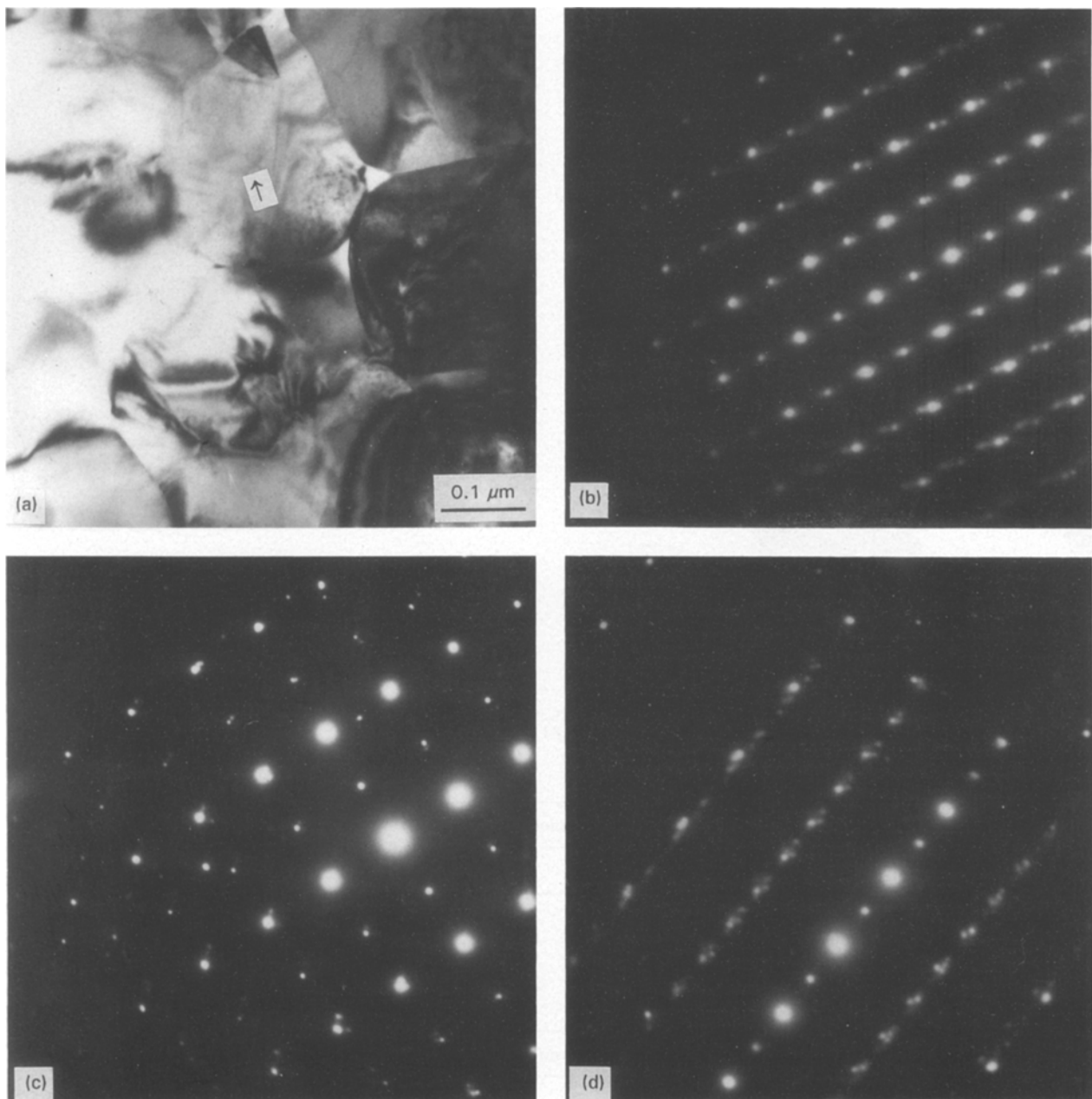


Figure 7 (a) The bright field image of the joint bonded at 1424°C for 30 min with $p/o = 3.17$; (b) corresponding $[01\bar{1}]_t$ selected area diffraction pattern; (c) corresponding $\{112\}_t$ selected area diffraction pattern; and (d) corresponding $\{210\}_t$ selected area diffraction pattern.

study [27], the decrease in the lattice parameters of the m- and t-ZrO₂ resulted from the effect of Ti⁴⁺ outweighed that due to Ca⁴⁺ in ZrO₂-CaO-TiO₂ multiphase ceramic. In addition, increasing amounts of titania also reduced the amounts of cubic phase, i.e. the amount of the monoclinic phase was increased. It is believed that yttrium tends to be dissolved into the glass as evidenced by the X-ray mapping in Fig. 6(f). The out-diffusion of yttrium may result in the loss of matrix strength and the decrease of the bending strength of the YSZ3-CTS-YSZ3 assembly.

On the basis of the STEM-EDX and X-ray mapping results, one may conclude the following: (1) the glass ingredients Ca, Ti, and Si penetrate into the YSZ3 matrix and redistribute in the grain boundary triple point; (2) element Ti diffuses into the ZrO₂ grain and causes a t → m phase transformation; and (3) element Y dissolves into CTS liquid and may form another compound in the CaO-TiO₂-SiO₂ system.

It should be pointed out that the roughness of the bonding surface also influences the bending strength. Samples with YSZ3 surface polished to 1 μm exhibit

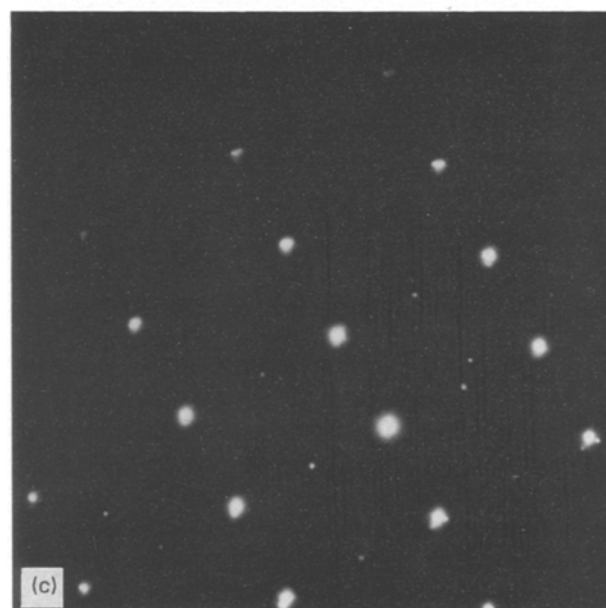
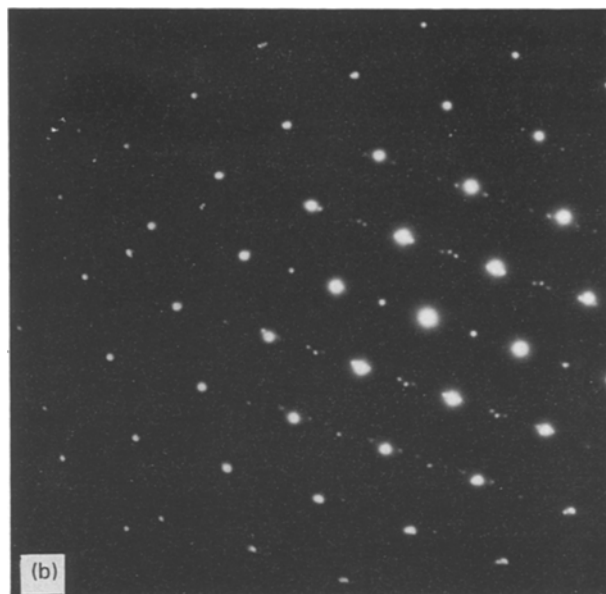
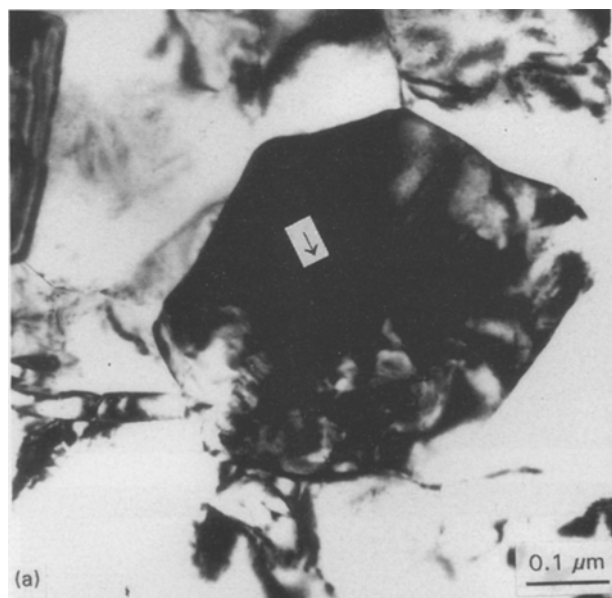


Figure 8 (a) The bright field image of the joint bonded at 1454 °C for 30 min with p/o = 3.17; (b) corresponding [0 1 1]_t selected area diffraction pattern; (c) corresponding {1 1 2}_t selected area diffraction pattern; and (d) corresponding {2 1 0}_t selected area diffraction pattern.

TABLE I (a) Compositions of grain and grain boundary near the joint. Samples were bonded at 1424 and 1454 °C for 30 min with p/o = 3.14. (b) Original compositions of CTS glass powder and YSZ3 bulk

Temperature (°C)		Compositions (mol %)				
		Si	Ca	Ti	Y	Zr
1424	grain boundary	54.62	34.94	0	3.53	6.92
	grain	0	0	2.07	7.91	90.02
1454	grain boundary	60.00	30.87	3.10	0.12	5.91
	grain	0	0	18.79	0	81.21

		Original compositions (mol %)				
		Si	Ca	Ti	Y	Zr
	CTS glass	56.22	21.86	21.92	0	0
	YSZ3	0	0	0	5.94	94.06

a bending strength about 50 MPa, which are higher than those of samples only ground by 240 SiC paper. The insert of Fig. 6b demonstrates this point. For a brazer with a high glass content such as $p/o = 3.17$, the glass remained in the joint, because the amount of liquid was too much to be consumed by crystallizing during cooling process for samples bonded at low temperature. It is argued that the bonding strength depends on the amount of the remaining glass, which has lower strength than ceramic does. In addition, if the CTS ceramic interlayer is too thick, the interlocking of ZrO_2 decreases and the bonding strength which depends predominantly on the mechanical properties of the CTS ceramics will decrease. Furthermore, when the samples are bonded at the higher temperature, the surface flow will increase, i.e. the viscosity of the CTS liquid decreases with increase of bonding temperature. The liquid will flow out of the joint and wet the free surface of the YSZ3 bulk under the weight of the upper YSZ3 bulk. This makes the $t \rightarrow m$ phase transformation on the free surface possible. Therefore, the bonding strength will further decrease if the bulk loses its strength due to the $t \rightarrow m$ transformation. As a result, the bonding strength reaches a maximum value at an optimum temperature for an appropriate p/o ratio as shown in Fig. 4.

4. Conclusions

1. $CaO-TiO_2-SiO_2$ (CTS) glass filler is employed for the bonding of yttria stabilized zirconia. Sandwiched YSZ3-CTS-YSZ3 bonding assemblies with slurry filler having various glass powder/organic ratio are investigated.

2. In the $p/o = 1.82$ case, the bonding strength increases initially and then decreases with the bonding temperature. It is attributed to the diffusion of the CTS liquid into ZrO_2 matrix and also to the $t \rightarrow m$ phase transformation of zirconia.

3. In the diffusion of CTS glass into the ZrO_2 matrix, Ca and Si are enriched in the grain boundary triple point, while Ti tends to diffuse into the grains to form a substitutional solid solution with zirconia. Besides, Y are unstable in ZrO_2 grains and tends to solute into CTS liquid to form a Ca-Ti-Y compound.

4. The $t \rightarrow m$ phase transformation is induced by the solid solution reaction in which the smaller Ti^{4+} ion substitutes the larger Zr^{4+} ion and makes the lattice parameter decreased. The small amount of monoclinic phase present in the tetragonal matrix is beneficial for mechanical properties because of the precipitation hardening and transformation toughening effect. Nevertheless, if too large, the strength will decrease due to the poor mechanical properties of the monoclinic zirconia.

5. There exists an optimal CTS glass slurry concentration (p/o) at about 1.82. If the ratio is too high, the excess CTS liquid will flow out of the joint to induce the $t \rightarrow m$ transformation on the free surface, which is

detrimental to the bonding strength. If the p/o ratio is too low, the amount of the CTS liquid is not enough to wet the bonded surface and an unbonded region in the joint is exposed, which results in a large deviation on the measured bonding strength.

Acknowledgement

The authors acknowledge the financial support of National Science Council, Taiwan, under contract No. NSC 81-0404-E009-610.

References

1. C. D. QIN, N. A. JAMES and B. DERBY, *Acta Metall. Mater.* **40** (1992) 925.
2. C. D. QIN and B. DERBY, *J. Mater. Res.* **7** (1992) 1480.
3. J. G. DUH, W. S. CHIEN and B. S. CHIOU, *J. Mater. Sci. Lett.* **8** (1989) 405.
4. J. G. DUH, Y. C. WU and B. S. CHIOU, *J. Mater. Sci.* **25** (1990) 2626.
5. Y. YOSHINO, *J. Am. Ceram. Soc.* **72** (1989) 1322.
6. X. M. XUE, Z. T. SUI and J. T. WANG, *J. Mater. Sci. Lett.* **11** (1992) 1514.
7. R. E. LOEHMAN and A. P. TOMSIA, *Acta Metall. Mater.* **40** (1992) S75.
8. N. IWAMOTO and H. YOKOO, *J. Mater. Sci.* **27** (1992) 441.
9. R. C. RATHNER and D. J. GREEN, *J. Am. Ceram. Soc.* **73** (1990) 1103.
10. N. IWAMOTO and H. YOKOO, *Engineering Fracture Mechanics* **40** (1991) 931.
11. T. NAGANO, H. KATO and F. WAKAI, *J. Mater. Sci.* **26** (1991) 4985.
12. S. BAIK, *J. Am. Ceram. Soc.* **70** (1987) c105.
13. P. F. BECHEER and S. A. HALEN, *Ceram. Bull.* **58** (1979) 582.
14. S. L. SWURTZZ, B. S. MAJUMDER, A. SKIDMORE and B. C. MUTSUDDY, *Mater. Lett.* **7** (1989) 407.
15. W. A. ZDANIEWSKI, P. M. SHAH and H. P. KIRCHNER, *Adv. Ceram. Mater.* **2** (1987) 204.
16. M. L. MECARTNEY and R. SINCLAIR, *J. Am. Ceram. Soc.* **68** (1985) 472.
17. S. M. JOHNSON and D. J. ROWCLIFFE, *ibid.* **68** (1985) 468.
18. R. C. DEVRIESS, R. ROY and E. F. QSBORN, *ibid.* **38** (1955) 158.
19. J. G. DUH, H. T. DAI and B. S. CHIOU, *ibid.* **71** (1988) 813.
20. TSK Ceramics Technical Bulletin, Toyo Soda Manufacturing Co. Ltd, No. Z-112 (1986).
21. F. F. LANGE, *J. Mater. Sci.* **17** (1982) 225.
22. N. CLAUSSEN and M. RUHLE, in "Advances in Ceramics, Vol. 3", edited by A. H. Heuer (The American Ceramic Society, Columbus, OH, 1988) pp. 137-152.
23. R. H. J. HANNINK, K. A. JOHNSON, R. T. PASCOE and R. C. GARVIE, *ibid.* pp. 116-136.
24. D. C. AGRAWAL, R. GOPALAKRISHNAN and D. CHAKRAVORTY, *J. Am. Ceram. Soc.* **72** [6] (1989) 912.
25. R. C. WEAST and M. J. ASTLE, editors "CRC Handbook of Chemistry and Physics" (CRC, Florida, 1980) pp. F-216-F-217.
26. P. RAMASWAMY and D. C. AGRAWAL, *J. Mater. Sci.* **22** (1987) 1243.
27. D. C. AGRAWAL, R. GOPALAKRISHNAN and D. CHAKRAVORTY, *J. Am. Ceram. Soc.* **72** (1989) 912.

Received 13 October 1993

and accepted 27 July 1994